

Vibrational Signatures in the Infrared Spectra of Single- and Double-Walled Carbon Nanotubes and Their Diameter Dependence

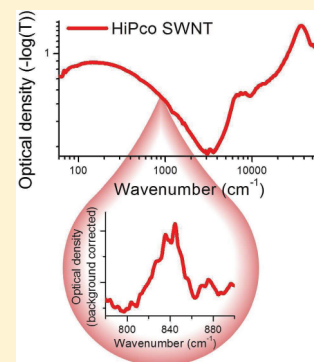
Á. Pekker,[†] Á. Botos,^{†,§} Á. Ruzsnyák,[‡] J. Koltai,[‡] J. Kürti,[‡] and K. Kamarás^{*,†}

[†]Research Institute for Solid State Physics and Optics, Hungarian Academy of Sciences, P.O. Box 49, H-1525 Budapest, Hungary

[‡]Department of Biological Physics, Eötvös Loránd University, Pázmány Péter sétány 1a, H-1117 Budapest, Hungary

ABSTRACT: While the vibrational features detected by Raman spectroscopy constitute an essential fingerprint of carbon nanotubes, the same is not true for infrared spectroscopy: studies are few, and agreement is scarce. In this paper, we study wide-range transmission spectra of a series of single-walled nanotube samples, differing in their diameter distribution. In all samples, distinct vibrational features could be detected in the mid-infrared region. We found a correlation between the frequency of the S_{11} electronic transitions and the 860 cm^{-1} vibrational band, leading to the conclusion that this vibrational mode hardens with increasing nanotube diameter. Our results are in accordance with density functional theory calculations. The vibrational features in double-walled nanotubes correspond to those of the isolated single-walled tubes of similar size.

SECTION: Nanoparticles and Nanostructures



Ever since the beginning of nanotube research, Raman spectroscopy has been the method of choice for investigating vibrational properties of carbon nanotubes. Although calculations never showed any infrared (IR) transitions to be forbidden, only spurious experimental activity exists regarding IR-active vibrations.^{1–5}

Here we report results obtained by infrared spectroscopy on a series of well-defined single-walled nanotube (SWNT) samples which differ in their composition regarding the mean diameter and diameter distribution of tubes. We find positive evidence in the IR spectra for vibrational transitions and observe the frequency of these vibrations to scale monotonically with the diameter of the tube ensembles, the opposite of the electronic transition frequencies. This type of diameter dependence is in agreement with recent density functional theory (DFT) calculations. In double-walled nanotubes (DWNT) prepared from C_{60} -filled tubes, the vibrational spectra correspond to the sum of the outer tube and that of narrow tubes with mean diameter similar to that of the inner tubes.

We investigated the transmission spectra of self-supporting nanotube films in detail. Prerequisite for this study were five well characterized⁶ commercial SWNT samples with varying diameter distribution (Table 1). The diameter of a nanotube determines most optical properties, notably the radial breathing mode (RBM) frequency in the Raman spectrum and the interband transitions between Van Hove singularities in the near-infrared/visible (NIR/VIS) and photoluminescence spectra. Our samples are free of substrate effects, and therefore we can compare the S_{11} transitions (which possess a known diameter dependence⁷) and the newly discovered vibrational transitions.

The wide-range spectra of all SWNT films are shown in the left panel of Figure 1. The interband transitions between Van Hove

Table 1. Mean Diameter Values and Diameter Distributions of the SWNT Samples Investigated

sample	mean diameter (nm)	diameter range (nm)
arc (P2)	1.42	1.24–1.59
laser	1.25	1.03–1.47
HiPco	1.08	0.79–1.25
CoMoCat CG	0.90	0.55–1.17
CoMoCat SG	0.76	0.55–0.96

singularities stand out in the NIR/VIS range and show the expected inverse dependence with diameter; however, in all spectra there are small but reproducible peaks in the vibrational region. An enlarged plot after baseline correction and scaling is presented in the right panel. We indicate three regions where vibrational structure is apparent for all samples: around 500 , 860 , and 1600 cm^{-1} . The latter two have been observed before, in the majority of previous studies.^{1–3} There has been one set of data reported,^{4,5} which is markedly different from all other studies, containing far more peaks. We also observe various other peaks in some of our samples in Figure 1, and restrict ourselves to the ones that appear in every kind of nanotube.

In the following, we concentrate on the peak around 860 cm^{-1} . This frequency is very close to the A_{2u} vibration of graphite^{8,9} at 868 cm^{-1} and is assigned on the basis of line groups¹⁰ by Dobardžić et al. to line group symmetry ${}_0A_0^-$ or ${}_0E_1^-$ in chiral nanotubes; ${}_0A_0^-$ in zigzag tubes, and ${}_0E_1^+$ in armchair tubes.

Received: July 4, 2011

Accepted: July 29, 2011

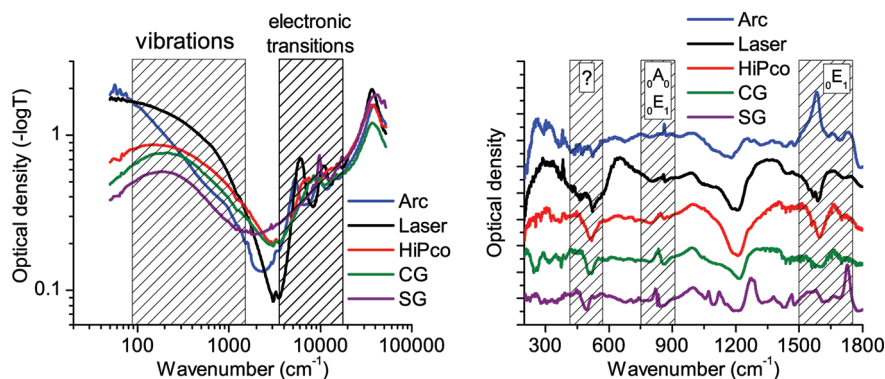


Figure 1. Left: Wide-range optical density of five types of SWNTs: arc, laser, HiPco, CoMoCat commercial grade (CG) and CoMoCat scientific grade (SG). Note the logarithmic frequency scale to emphasize the region of vibrational excitations. Right: The vibrational IR part of the spectra, after baseline correction and scaling.

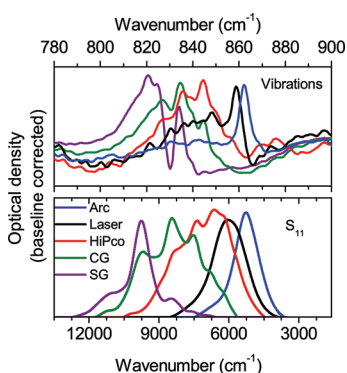


Figure 2. Top: the 860 cm^{-1} vibration peaks; bottom: the S_{11} electronic transitions for the samples studied. Samples are characterized by the color code. All curves have been baseline corrected and scaled for better visibility. Note that the frequency scale is opposite for the top and bottom curves: electronic transitions increase in frequency for decreasing diameter, vibrational excitations increase in frequency for increasing diameter.

The atomic displacements in this vibrational mode have only radial components, similarly to the RBM. The only difference is in the parity. While the RBM is even with respect to the z -reversal transformation (${}_{0}A_{0}^{+}$), the IR active mode is odd (${}_{0}A_{0}^{-}$), meaning that the neighboring atoms are moving in the opposite direction.¹⁰ Such a motion resembles a twisting mode, in contrast to the pure stretching character of the RBM. These modes have opposite diameter dependences, based on simple geometrical arguments. The frequency of the ${}_{0}A_{0}^{-}$ mode is expected to decrease with diameter.

In Figure 2 we compare the above-mentioned peak (which, for simplicity, we call the 860 cm^{-1} peak regardless of the diameter dependence) to the S_{11} interband transitions for all samples investigated. The latter is known to scale with the inverse diameter, therefore we show these data on a reversed scale. In both cases, the width and line shape of the modes is determined by the diameter distribution of the samples. It is obvious from the plot that a very similar diameter distribution is reflected in both frequency regions.

Figure 3 contains the calculated and measured spectra around 860 cm^{-1} for three samples consisting of few types of tubes so that the distribution could be modeled in order to compare the theoretical and experimental values. The theoretically determined frequencies of one-dimensional IR active phonon modes were plotted with Lorentzian broadening. The line widths and intensities

were fitted to the measured curve in the case of CoMoCat CG and SG. In the HiPco case, all 24 types of tubes in the diameter range were taken into account with the same line width (1.1 cm^{-1}), and the intensity was weighted by a Gaussian distribution around 1 nm with variance 0.2 nm . The qualitative agreement is rather obvious and can be improved further by adjusting the natural line widths. Theory also predicts increasing frequency of the IR modes with increasing diameter, saturating at the graphene value.

Additional evidence linking the 860 cm^{-1} peak to the nanotube vibrations comes from the spectra of peapod-derived DWNTs (Figure 4). These tubes have been prepared from C_{60} -filled single-walled P2 nanotubes and annealed in order to form an inside nanotube.¹¹ These inside tubes are expected to contain no amorphous carbon or catalyst particles and are therefore much closer to pristine material than the ones produced from carbon precursors.¹²

We compare four spectra in Figure 4: the original P2, a P2 after annealing without filling (to exclude extrinsic heating effects; marked P2 REF), a DWNT prepared from P2 by filling with C_{60} ,¹¹ and a CoMoCat CG sample. The diameter distribution of the latter is somewhat broader than the inner tubes formed from P2, considering the van der Waals distance of the inner and outer tubes.¹³ High-resolution Raman spectra of very similar DWNTs^{14,15} have shown that the RBMs of the inner tubes correspond to those of CoMoCat SWNTs. The spectra in Figure 4 show clearly that (a) no change in the vibrational peak occurs on annealing alone; and (b) the spectrum of the double-walled tube contains both the outer tube spectrum and that of a nanotube sample with diameter distribution close to the inner tubes. Indeed, the distribution of the lower-frequency peak in the DWNT sample is narrower than that of the CoMoCat CG, which is expected taking into account the difference in diameter distribution of the CoMoCat sample and the one calculated for inner tubes.¹⁶

We regard the data presented in Figure 4 as strong proof for the peak being of vibrational origin in the nanotubes. It is interesting that the vibrations of the inner tubes are visible through the walls of the outer tubes, whereas this is not observed in fullerene peapods^{11,17} and other systems.¹⁸

EXPERIMENTAL METHODS AND CALCULATION DETAILS

Samples were received from commercial suppliers (arc: Carbon Solutions, Inc.;¹⁹ laser: Tubes@Rice; HiPco: Carbon

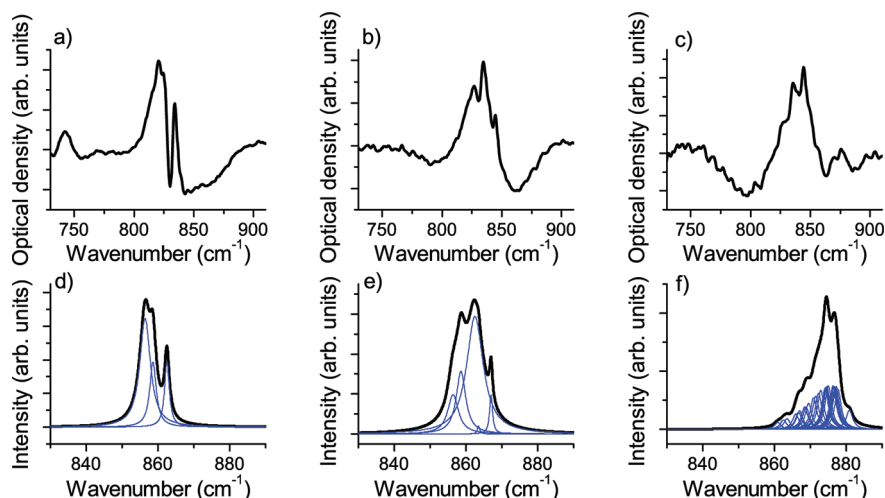


Figure 3. Measured and calculated spectra of three types of nanotubes: CoMoCat SG (panels a,d), CoMoCat CG (panels b,e), and HiPco (panels c,f). Blue curves are calculated data for individual nanotubes.

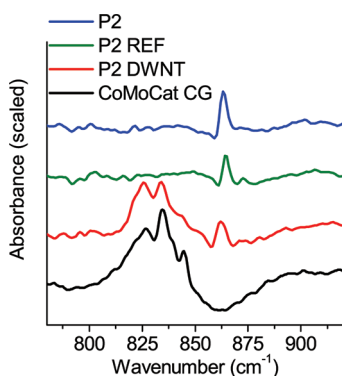


Figure 4. The 860 cm^{-1} vibration peaks in DWNTs and their constituents. The spectrum of the DWNT contains the features of both the outer tube and a sample with approximately the same mean diameter as the inner tubes. Curves have been baseline corrected like the curves in Figure 1 and scaled for better visibility.

Nanotechnologies, Inc.; CoMoCat: Southwest Nanotechnologies²⁰). The laser sample underwent acid reflux in order to remove catalyst particles and is considered to be heavily doped as a result. Self-supporting films were prepared by vacuum filtration.²¹ Spectra were taken by various spectrometers: a Bruker IFS 66v in the far- and mid-infrared, a Bruker Tensor 37 in the mid- and near-infrared, and a JASCO v550 grating spectrometer in the visible-ultraviolet (VIS/UV). We used a standard transmission arrangement with normal incidence. Spectral resolution was typically 2 cm^{-1} in the far- to near-infrared range, and 1 nm in the VIS/UV range. Baseline correction was done by a polynomial fit for the wide-range spectra to arrive at the vibrational region (transition between left and right panel of Figure 1), and additionally, a linear background was subtracted in the narrow range of the 860 cm^{-1} vibration (Figure 2, upper panel, and Figure 4).

First-principles calculations using DFT have been performed for both geometry optimization and vibration analysis. The Vienna ab initio simulation package (VASP)²² was used with a plane-wave basis set employed within the framework of the projector augmented-wave method. The plane-wave cutoff energy was set to 500 eV . Optimization was performed until all force components

fell below $3\text{ meV}/\text{\AA}$. A k -point set of $1 \times 1 \times 1 - 1 \times 1 \times 20$ Γ -centered Monkhorst-Pack grid (depending on the number of atoms in the unit cell) was used for geometry optimization. We have calculated the dynamical matrix and solved its eigenvalue problem numerically. Identification of the IR active modes was based on symmetry analysis according to the line group method.^{10,23} It is very important to use the correct symmetry, as was pointed out in ref 24. All semiconducting tubes were studied in the diameter range between 0.3 and 1.1 nm . Similar calculations have been performed for one chiral and a few types of zigzag nanotubes.²⁵ They showed that, although the displacements are radial in the oA_0^- mode, they induce a dipole in the axial direction. Summing them along the tube axis results in a small but measurable dipole moment.

AUTHOR INFORMATION

Corresponding Author

*E-mail: kamaras@szfki.hu.

Present Addresses

⁵School of Chemistry, University of Nottingham, University Park, Nottingham NG7 2RD, United Kingdom.

ACKNOWLEDGMENT

The research leading to these results has received funding from the European Community's Seventh Framework Programme FP7/2007-2013 under grant agreement No. 215399 and from the Hungarian Scientific Research Fund (OTKA) Nos. K75813 and K81492.

REFERENCES

- (1) Kastner, J.; Pichler, T.; Kuzmany, H.; Curran, S.; Blau, W.; Weldon, D. N.; Delamesiere, M.; Draper, S.; Zandbergen, H. Resonance Raman and Infrared Spectroscopy of Carbon Nanotubes. *Chem. Phys. Lett.* **1994**, *221*, 53–58.
- (2) Kuhlmann, U.; Jantoljak, H.; Pfänder, N.; Bernier, P.; Journet, C.; Thomsen, C. Infrared Active Phonons in Single-Walled Carbon Nanotubes. *Chem. Phys. Lett.* **1998**, *294*, 237–240.
- (3) Bantignies, J.-L.; Sauvajol, J.-L.; Rahmani, A.; Flahaut, E. Infrared-Active Phonons in Carbon Nanotubes. *Phys. Rev. B* **2006**, *74*, 195425.

(4) Kim, U. J.; Liu, X. M.; Furtado, C. A.; Chen, G.; Saito, R.; Jiang, J.; Dresselhaus, M. S.; Eklund, P. C. Infrared-Active Vibrational Modes of Single-Walled Carbon Nanotubes. *Phys. Rev. Lett.* **2005**, *95*, 157402.

(5) Kim, U. J.; Furtado, C. A.; Liu, X. M.; Chen, G.; Eklund, P. C. Raman and IR Spectroscopy of Chemically Processed Single-Walled Carbon Nanotubes. *J. Am. Chem. Soc.* **2005**, *127*, 15437–15445.

(6) Pekker, Á.; Kamarás, K. Wide-Range Optical Studies on Various Single-Walled Carbon Nanotubes: Origin of the Low-Energy Gap. *Phys. Rev. B* **2011** in press (arXiv:1101.4586).

(7) Kataura, H.; Kumazawa, J.; Maniwa, Y.; Umezū, I.; Suzuki, S.; Ohtsuka, Y.; Achiba, Y. Optical Properties of Single-Wall Carbon Nanotubes. *Synth. Met.* **1999**, *103*, 2555–2558.

(8) Jeon, G. S.; Mahan, G. D. Microscopic Origin of Infrared Activity in Graphite. *Phys. Rev. B* **2005**, *71*, 184306.

(9) Jeon, G. S.; Mahan, G. D. Theory of Infrared-Active Phonons in Carbon Nanotubes. *Phys. Rev. B* **2005**, *72*, 155415.

(10) Dobardžić, E.; Milošević, I.; Nikolić, B.; Vuković, T.; Damnjanović, M. Single-Wall Carbon Nanotubes Phonon Spectra: Symmetry-Based Calculations. *Phys. Rev. B* **2003**, *68*, 045408.

(11) Botka, B.; Pekker, Á.; Botos, Á.; Kamarás, K.; Hackl, R. A Systematic Study of Optical and Raman Spectra of Peapod-Based DWNTs. *Phys. Status Solidi B* **2010**, *247*, 2843–2846.

(12) Pfeiffer, R.; Kuzmany, H.; Kramberger, C.; Schaman, C.; Pichler, T.; Kataura, H.; Achiba, Y.; Kürti, J.; Zólyomi, V. Unusual High Degree of Unperturbed Environment in the Interior of Single-Wall Carbon Nanotubes. *Phys. Rev. Lett.* **2003**, *90*, 225501.

(13) Bandow, S.; Takizawa, M.; Hirahara, K.; Yudasaka, M.; Iijima, S. Raman Scattering Study of Double-Wall Carbon Nanotubes Derived from the Chains of Fullerenes in Single-Wall Carbon Nanotubes. *Chem. Phys. Lett.* **2001**, *337*, 48–54.

(14) Simon, F.; Pfeiffer, R.; Kuzmany, H. Temperature Dependence of the Optical Excitation Lifetime and Band Gap in Chirality Assigned Semiconducting Single-wall Carbon Nanotubes. *Phys. Rev. B* **2006**, *74*, 121411(R).

(15) Kuzmany, H.; Plank, W.; Pfeiffer, R.; Simon, F. Raman Scattering from Double-Walled Carbon Nanotubes. *J. Raman Spectrosc.* **2008**, *39*, 134–140.

(16) The diameter distribution of the inner tubes is limited on the low-diameter side by the size of the C₆₀ molecule and on the high-diameter side by ($d_{\text{max}} - 0.68$) nm, where d_{max} is the maximum of the P2 diameter distribution. The distribution of CoMoCat CG is broader than this range, with approximately the same median value.

(17) Botos, Á.; Khlobystov, A. N.; Botka, B.; Hackl, R.; Székely, E.; Simándi, B.; Kamarás, K. Investigation of Fullerene Encapsulation in Carbon Nanotubes Using a Complex Approach Based on Vibrational Spectroscopy. *Phys. Status Solidi B* **2010**, *247*, 2743–2745.

(18) Kazachkin, D. V.; Nishimura, Y.; Witek, H. A.; Irle, S.; Borguet, E. Dramatic Reduction of IR Vibrational Cross Sections of Molecules Encapsulated in Carbon Nanotubes. *J. Am. Chem. Soc.* **2011**, *133*, 8191–8198.

(19) Carbon solutions, Inc. Homepage. <http://www.carbonsolution.com> (accessed July 2011).

(20) Southwest Nanotechnologies (SWeNT) Homepage. <http://www.swentnano.com> (accessed July 2011).

(21) Wu, Z. C.; Chen, Z. H.; Du, X.; Logan, J.; Sippel, J.; Nikolou, M.; Kamarás, K.; Reynolds, J. R.; Tanner, D. B.; Hebard, A. F.; Rinzler, A. G. Transparent, Conductive Carbon Nanotube Films. *Science* **2004**, *305*, 1273–1276.

(22) Kresse, G.; Furthmüller, J. Efficient Iterative Schemes for Ab Initio Total-Energy Calculations Using a Plane-Wave Basis Set. *Phys. Rev. B* **1996**, *54*, 11169.

(23) Damnjanović, M.; Milošević, I.; Vuković, T.; Sredanović, R. Full Symmetry, Optical Activity, and Potentials of Single-Wall and Multiwall Nanotubes. *Phys. Rev. B* **1999**, *60*, 2728–2739.

(24) Alon, O. E. Number of Raman- and Infrared-Active Vibrations in Single-Walled Carbon Nanotubes. *Phys. Rev. B* **2001**, *63*, 201403.

(25) Zhou, J.; Dong, J. Infrared Properties of Single-Walled Carbon Nanotubes Calculated from First Principles. *J. Appl. Phys.* **2010**, *107*, 024306.